International Journal of Environmental Sciences
ISSN: 2229-7359
Vol. 11 No. 18s, 2025
https://theaspd.com/index.php

"Integrated Synthetic And In Silico Investigation Of Indane-1,3-Dione Derivatives As Potent Inhibitors Of Plasmodium Falciparum LDH"

Nitin Londhe[1], Karthickeyan Krishnan[2]
[1]Research Scholar, School of Pharmaceutical Sciences, Vels Institute of Science, Technology and Advanced Studies (VISTAS), Pallavaram, Chennai, Tamil Nadu, 600117, India
[2]Professor and Head, Department of Pharmacy Practice, School of Pharmaceutical Sciences, Vels Institute of Science, Technology & Advanced Studies, Pallavaram, Chennai-600117, Tamilnadu

Abstract
In the present study, 15- Indane 1.3 dione derivatives were designed and docking studies were performed using PyRx tool by targeting Pf-LDH(1LDG) and Aspartic protease plasmepsin II (1LEE) as antimalarials.The drug likeness and ADME analysis were performed on the developed Indane 1.3 dione derivatives. The compounds with the best ADME score were then assessed by docking them against the 1LDG and 1LEE targets. Assay were performed to validate in-vitro antimalarial medication for the Plasmodium falciparum sensitive to chloroquine (3D-7).Comparing Pf-LDH(1LDG) to 1LEE, the latter target has poorer binding interactions with the amino acids Val141,Lys129,Trp128,Asp130,Asp190,Leu324,Pro181,Tyr266,Ile322,Tyr309,Thr183 and Asn263. When it comes to Schizonts, Compounds XI, XII, and XIV have demonstrated half-maximum levels of inhibition (IC_{50}) values less than 0.5 μM (or <500 nM). Compounds I, V, VII, VIII, X, XIII, and XV displayed moderate activity according to the IC_{50} values, while compounds II, III, IV, VI, and IX demonstrated less activity.Additionally, against a strain resistant to chloroquine, three compounds exhibited IC_{50} values that range from 9.23 to 9.56 μg/ml. Compounds XI, XII, and XIV were discovered to be effective against the Plsmodium falciparum that is sensitive to chloroquine (3D-7).
Keywords: *Indane 1.3 dione, Antimalarial, Docking, ADMET, Pf-LDH, Plasmepsin- II*

INTRODUCTION:

In 2021, 84 countries where malaria is prevalent, including French Guiana, recorded 247 million cases of malaria worldwide. The WHO African Region accounted for the majority of this increase. In 2015, which is regarded as the baseline year of the global technological plan for combating malarial parasite infection, there were an approximate 230 million incidences of malaria.The COVID-19 pandemic-related service disruptions in 2020 were linked to the rise[1].Pregnant women and children account for over a million deaths each year. The genus Plasmodium, which causes malaria, is a parasitic and hematologic disease spread via the female Anopheles mosquito's bites vectors carrying the infection[2-3]. The parasite Plasmodium falciparum causes malaria has a problem developing drug resistance, and the lack of a vaccine has made it necessary to look for new pharmacological skeletons with unique modes of action and the capacity to target novel protein targets[4-5]. TP. falciparum is the most deadly parasite, with the highest rates of fatality and morbidity[6].It has been determined that Human malaria is caused by five different species of Plasmodium: P. ovale, P. vivax, P. malariae, P. knowlesi, and P. falciparum. The most prevalent and virulent of them is Plasmodium falciparum[7].Many of the antimalarial medications that were once successful have become ineffective due to widespread drug resistance, and developing new drug combinations for chemotherapy is now necessary To stop the malarial parasite from quickly developing resistance to artemisinin and its derivatives, currently available medications such as mefloquine, quinine, chloroquine, and artemisinin-based combination therapy have been used against the parasite. ACTs have been the primary treatment for falciparum malaria up to the previous eighteen years[8]. Following plasmodium parasite dispersal, the parasites quickly entered the bloodstream and entered the liver, where they infected hepatic cells. Thousands of merozoite cells were finally produced by it after it multiplied. Following their release into bloodstream, merozoites infect RBCs, it causes malaria infection[9].The antimalarial medications function by preventing the synthesis of hemozoin, which creates free radicals inside the digestive vacuoles or hemoglobin, which is hydrolyzed into globin and

heme parts inside the digestive vacuoles[10]. Potential medications that are already on the market target the diverse family of plasmodium enzymes, which includes falcipains, aminopeptidases, and plasmepsins (PMs). These enzymes have a role in hemoglobin hydrolysis in human hosts as well as other vital activities such erythrocyte invasion and rupture[11-16].Proton donors and other acceptors hydrolyze the amide group of peptide bonds in proteins, and the two aspartic acid residues that comprise PMs are these donors[17].Aspartic protease, metalloproteases (falcilysin), and cysteine proteases (falcipain-1, -2, and -3) are responsible for the breakdown of hemoglobin[18].A set of essential enzymes in the malarial parasite's life cycle, these target proteins have ten distinct isoforms, and inhibiting plasmepsins causes the parasite to die[19-21].The antimalarial medication artemisinin, which is presently on the market, inhibits the activity of both plasmepsin I and plasmepsin II[22].The glycolytic pathway has drawn a lot of attention in the hunt for substitute medications due to its pivotal function in producing adenosine triphosphate (ATP), which is necessary to power cellular functions in the majority of protozoan parasite life cycles. One of the crucial and promising enzyme targets found in the glycolytic cycle of parasites, lactate dehydrogenase (LDH) controls the production of ATP, which drives biological mechanisms in most The life cycles of parasitic protozoa[23].Another target for antimalarial medications is malarial lactate dehydrogenase, which is necessary in proliferation and parasite's survival[24].Throughout P. falciparum's anaerobic erythrocytic stages of life, it serves to regulate the generation of cellular constituent ATP by catalysis, which results in the The last stage of the glycolytic process involves the conversion of lactate to pyruvate[25]. Pf-LDH enzyme might be desirable target for development and discovery of anti-malarial drugs since it inhibits Pf-LDH growth and causes parasite death[26]. In order to generate, find, and analyze drug candidates and related physiologically active compounds, Insilico studies that use computer-aided drug design (CADD) techniques such virtual screening, pharmacophore modeling, molecular docking, and dynamic simulation are now commonly employed[27].Molecular docking is essential when using the structure-based drug design (SBDD) technique since it forecasts the ideal binding posture of a molecule with the target binding affinity and active sites[28]. Important information on whether a molecule can become a good candidate with desirable attributes early in the process of development is provided by in-silico physicochemical property data of a series of compounds under research, such as log P, TPSA, size, solubility, saturation, and flexibility[29]. The objectives of this study were to predict ligand binding interactions and their drug properties, as well as to perform molecular docking simulations using PyRx virtual screening software and to predict ADME and drug-likeness on the derivatives of indane 1,3 diones on two targets: lactate dehydrogenase (Pf-LDH) and Aspartic protease plasmepsin II protein. The results of the investigation are displayed here.

2. MATERIALS AND METHODS

2.1 Ligand Preparation

Chem sketch Ultra v.7.0.1 is used to sketch the chemical structures of fifteen created compounds in cdx format. These are subsequently translated to SDF format. A database of fifteen tiny compounds is created internally. Atomic coordinates were made up using the online Open Babel GUI program by switching to the pdbqt format. Standard drug structures were acquired from Pubchem in 3D format and saved as SDF files. Open Babel was then used to convert the SDF file to pdb format[30-31].

2.2 Protein Preparation

The Protein Data Bank provided 3D crystal structures of aspartic protease plasmepsin II protein with accession code 1LEE and Pf-LDH (PDB ID: 1LDG) in complex with NADH and the substrate oxamate for this study[32].The X-ray diffraction method was utilized to experimentally solve both structures, yielding resolutions of 1.90 A^0 and 1.74 A^0 for 1LEE and 1LDG, respectively. The docking evaluation was saved in PDB format and was obtained from the protein data bank (PDB ID: 1LEE). Co-crystallized ligand RS367 and two related chains, chains A and B, are present in the 1LEE PDB structure. Chain A has been chosen for additional docking. The dimensions of 25 × 25 × 25 A^0 are the grid size that covers the entire binding site region[33].The BIOVIA Discovery Studio was established to visualize the structure. For preparation of the protein, undesirable chains were cut off, and the water molecules and het atoms from both proteins' A chains were also eliminated[34].

2.4 Molecular Docking

The PyRx tool, Autodock vina software, is employed to carry out Ligand-enzyme docking simulations to determine the optimal alignment of a chemical that binds to the enzyme of interest. To locate The PyRx 8.0 tool's Autodock 4.2 docking studies perform bind free energy computations to determine the optimal ligand-molecule binding design to the target's active site area[35]. The ideal protein-ligand complex was found using the values of the minimal binding energy. Vina Wizard was used for molecular docking, while Discovery Studio was used to view and analyze the bonds involved in the interactions. The creation of new therapeutic medicines depends on our ability to comprehend the interactions between molecules that occur between molecules of ligands and enzymes. Accelerating Discovery Studio 3.5, the drug-receptor interactions are displayed in terms of three-dimensional structure.

2.5 Structural assessment of the protein

Using the online webserver Pdbsum database for both retrieved proteins, Ramchandran plots—which show every type of residue with Chi1-Chi2 plots, Main chain parameters, Residue properties, Side-chain parameters, protein main-chain bond angles, bond lengths, RMS distances, and distorted geometry—were exclusively used to analyze for input atoms[36].

2.6 In-Silico ADME/Pharmacokinetics Prediction

SwissADME, an online webserver program, accustomed to analyze the chemical and physical ADME characteristics of produced bioactive compounds (http://www.swissadme.ch)[37-38].Figure 1 displays the Indane 1, 3 dione derivatives bioavailability radar. Drug similarity parameters can be quickly assessed thanks to bioavailability radar[38].Six physicochemical factors were investigated in total: particle size, drug lipophilicity, polarity, flexibility, solubility, and saturation[39]. Researchers can evaluate a synthetic the drug-likeness of the chemical and its possible oral absorption in the body using the bioavailability radar[40].The pink area represents each property's ideal range. A boiled-egg chart that examines the ADME behavior of each drug under inquiry independently is produced by the SwissADME web server. The generated model provides information on BBB permeability and passive HIA. Two crucial parameters that are graphically displayed are brain access (BBB) and gastrointestinal absorption (HIA) by passive diffusion. BOILED-Egg[41].Additionally, they forecast the likelihood that the synthetic compound will function as either substrate or non-substrate of the permeability glycoprotein by utilizing most significant ATP transporter members, Because of the efflux mechanism's limited entry across target cells, the ATP parameter determines drug resistance. It forecasts whether a medication will exhibit drug resistance as a result of reduced access to the target cells via the efflux pump transport mechanism[42-43].The results of the boiled-egg and bioavailability radar plots are explained in table 3. Based on this discovery, Lipinski's rule of five is followed by all Indane 1, 3 dione derivatives. The requirements of Ro5 criteria are as follows: (i) Molecular weight must be less than or equal to 500 daltons (ii) Number of Hydrogen bond donors must be less than or equal to 5; iii) Number of Hydrogen bond acceptors must be less than or equal to 10; (iv) Log p-value (lipophilicity) must be less than or equal to 10; and (v) Molar refractivity must be between 40 and 130[44].

2.7 Synthesis of 2-(arylmethylene)-(1H)-indane-l,3-(2H)-diones

The derivatives that were previously described in our work were created by starting with an ethanolic solution of indane-l,3-dione and treating it with various aromatic aldehydes while piperidine was present to make 2-(arylmethylene)-(1H)-indane-l,3-(2H)-diones[45].

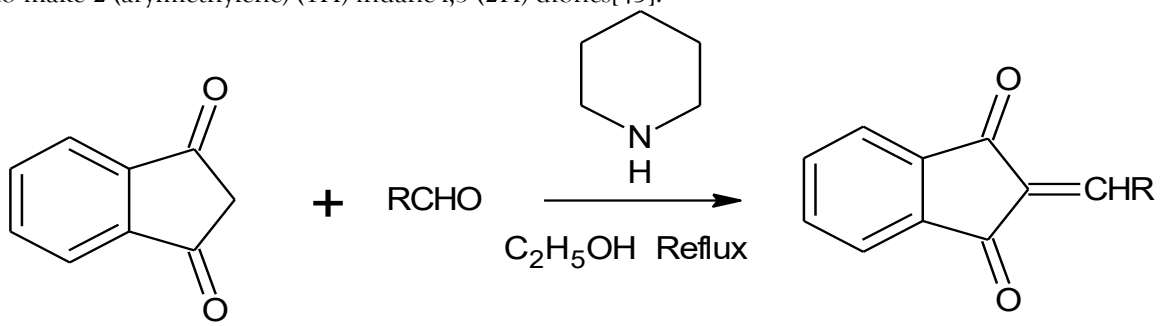

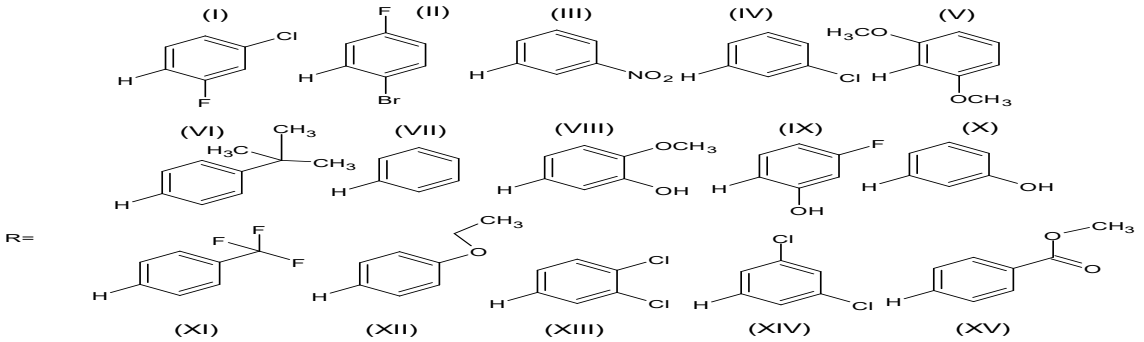

Fig 1: Reaction scheme of 2-(aryl methylene)-(1H)-indane-l,3-(2H)-diones derivatives

2.8 In-Vitro Antimalarial Activity[46]

It was done by **SMI assay**, and involved the following steps:

1. The synthesized compounds I through XV (1 mg/mL) were dissolved in 100 µL of DMSO and 900 µL of growth medium to create stock solutions.
2. RPMI 1640 medium was used to dilute this in order to get various medication concentrations. Dispensing these dilutions into 96-well microplates with a flat bottom was done.
3. Only culture media was present in the negative control wells.
4. After aliquoting the synchronized cultures into the plates and incubating them at 37 °C, the final haematocrit of 5% and the parasite of 1% were added.
5. Following a 24- to 30-hour culture, growth was seen.
6. Following the confirmation of schizont development, each well's blood was smeared.
7. Methanol was used to repair all of the slides.
8. The number of schizonts per 200 parasites in the asexual stage was measured. The test wells and control wells' values were contrasted.
9. Using HN-NonLin V1.1, the IC_{50} of each chemical was finally found.
10. The standard of excellence was chloroquine.

RESULTS AND DISCUSSION

An evaluation of the protein's structure

Fig. 2 displays the study of the Ramachandran plot.Tables 1 and 2 show the G-factors and Ramachandran Plot statistics for proteins 1LEE and 1LDG. A property's degree of unusualness or out-of-the-ordinaryness can be determined using the G factor. G factor levels below -0.5 are considered odd, and values below -1.0 are considered extremely unusual. The G factor values for 1LEE and 1LDG in this investigation were determined to be -0.08 and 0.34, respectively.

Table 1: Protein G-Factors and RamachandranPlot Statistics: 1LEE

Plot statistics			**G-Factors**		
	No. of residues	**Percentage**	**Parameter**	**Score**	**Average Score**
Areas Most Preferred [A, B, L]	246	85.7%*	Dihedral angles: distribution of phi-psi	- 0.49	
Extra permitted areas[a,b,l,p]	31	10.8%	Chi1-chi 2 distribution	- 0.37	
Generously permitted areas[~a,~b,~l,~p]	6	2.1%	Chi1 only	- 0.02	
Disallowed regions [XX]	4 1	4%*	Chi3 & chi4	0.13	
Non-proline and Non-	287	100.0%	Omega	0.21	
End	2		covalent forces:-		-0.16
Glycine	26		bond lengths		0.20
Proline	16		bond angles		-0.11
Total nos	331		Overall Average		-0.08

Table 2: Ramachandran Plot statistics and G-Factors for protein: 1LDG

Plot statistics			G-Factors		
	No. of residues	Percentage	Parameter	Score	Average Score
Areas Most Preferred [A, B, L]	253	92	Dihedral angles: distribution of phi-psi	- 0.04	
Extra permitted areas[a,b,l,p]	21	7.6	Chi1-chi 2 distribution	0 .16	
Generously permitted areas[~a,~b,~l,~p]	0	0.0	Chi1 only	0 .11	
Disallowed regions [XX]	1	0.4	Chi3 & chi4	0 .41	
Non-proline and Non-glycine	275	100.0	Omega	0 .49	
End	2		covalent forces		0.22
Glycine	26		bond lengths	0 .62	
Proline	12		bond angles	0.43	0.51
Total no	**315**		**Overall Average**		**0.34**

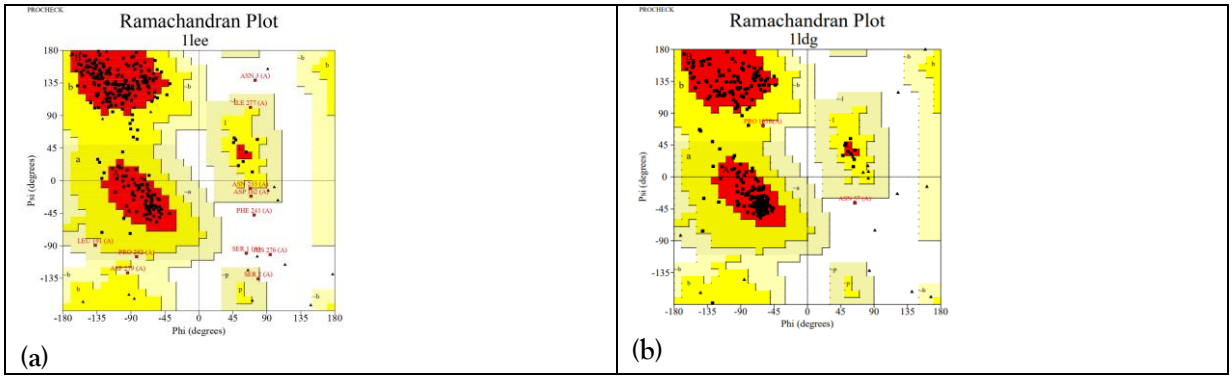

Fig. 2: Ramchandran Plot of proteins (a) Aspartic protease plasmepsin II(PDB:1LEE) (b) Plasmodium falciparum lactate dehydrogenase (Pf-LDH) (PDB:1LDG)

In-Silico ADME/Pharmacokinetics Prediction

The physicochemical space of the egg yolk indicates a likelihood of Blood Brain Barrier permeability, while egg white indicates a high likelihood of HIA absorption. The molecule's poor brain penetration was indicated by the low absorption in the gray region seen outside the brain. In this instance, the point is red if the molecule is not a substrate of P-glycoprotein (PGP−) and blue if the molecule is actively being gastro-efluxed by P-glycoprotein (PGP+).The projected fate of the produced molecule (III) in Figure 3 is that it will be absorbed and not breach the blood-brain barrier (beyond the egg) or undergo active efflux (red dot).

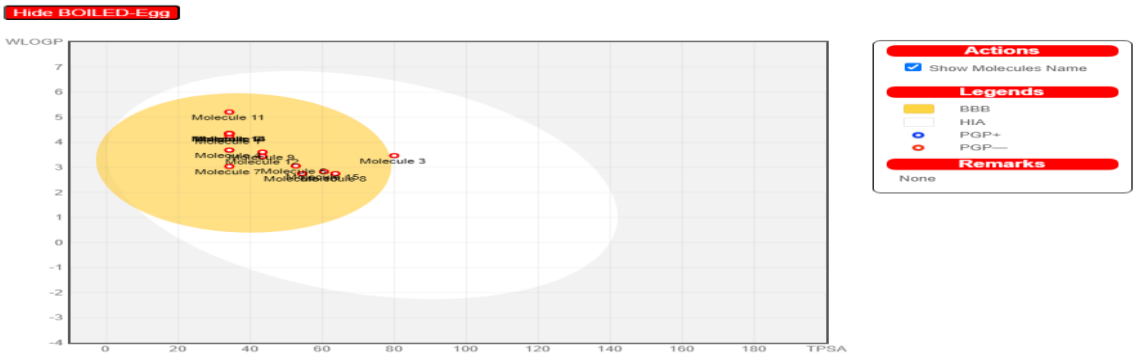

Figure 3. A boiled-egg diagram representing the bioactive substances under study

Compound III did not violate any of the examined parameters, as indicated by the bioavailability radar chart (Table 3). In contrast, all other compounds violated the unsaturation parameter due to their low fraction of sp3 carbons.

Table 3. Bioavailability radar graphic for bioactive compounds: the appropriate physicochemical space for oral bioavailability is shown by the colored zone

Comp-I	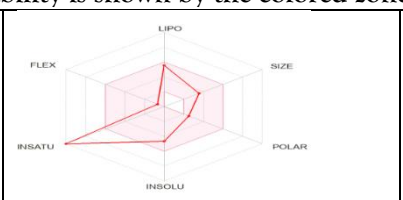	**Comp-IX**	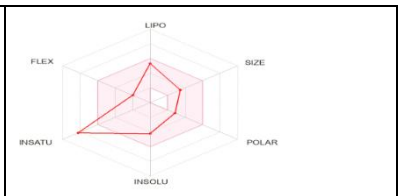
Comp-II	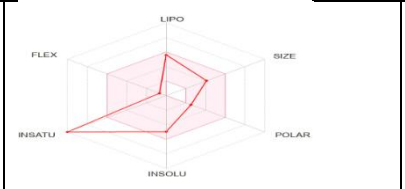	**Comp-X**	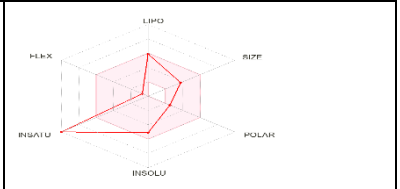
Comp-III	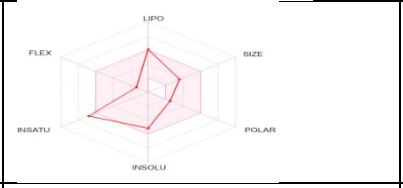	**Comp-XI**	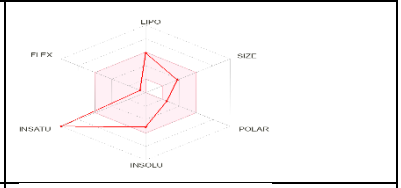
Comp-IV		**Comp-XII**	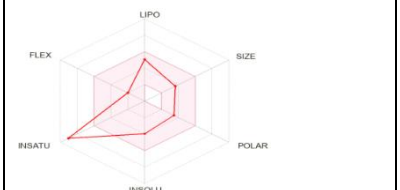
Comp-V	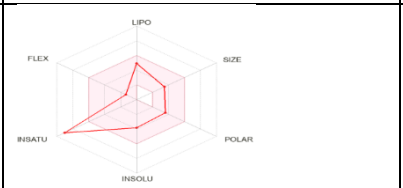	**Comp-XIII**	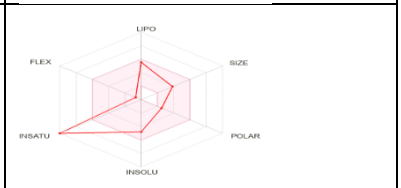
Comp-VI	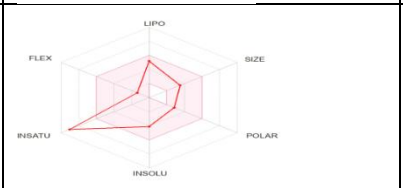	**Comp-XIV**	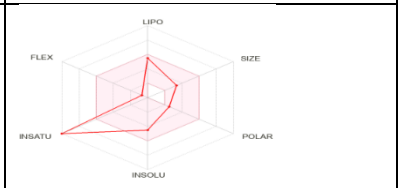
Comp-VII	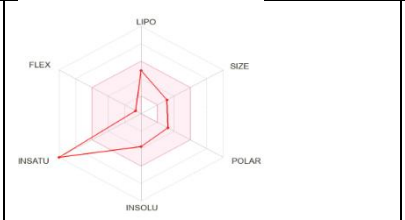	**Comp-XV**	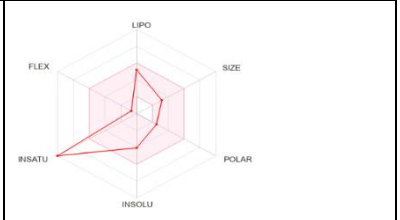
Comp-VIII	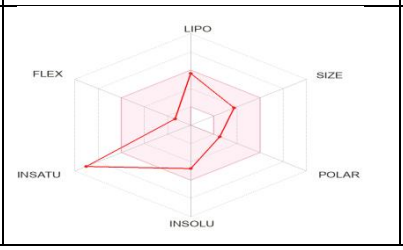		

Thus, it can be inferred that each of the compounds will have good intestinal absorption, as indicated by the boiled-egg chart's visual result for this class of compounds (Figure 3). Only compounds III, however, are anticipated BBB penetrant (with in yolk), suggesting that would have detrimental effects on central nervous system. However, it is not anticipated that the remaining derivatives I, II, IV, and V will pass through the BBB. All the investigated derivatives are unexpected to be susceptible according to the active efflux P-gP pathway, as their red colors suggest. When taking into account the permeability glycoprotein (P-gp) feature.

Drug likeness

Lipinski's parameters were used to assess drug likeness of 15 derivatives of Indane 1.3 dione, along with additional parameters listed Table 4.

Table 4: Prediction of Lipinski's rule for best docked compounds

Comp. No	Lipinski's Measurements					Additional Factors	
	M.W. (<500Da)	Log P (<5)	Hydrogen bond acceptor (< 10)	Hydrogen bond donor (< 5)	Lipinski's Violations	Topological polar surface area (< 140 Å^2)	N Rot B (< 10)
I	331.14	3.850	3	0	0	34.140	1
II	293.28	3.930	3	0	0	34.140	1
III	268.7	2.400	4	0	0	79.960	2
IV	280.68	3.550	2	0	0	34.140	1
V	268.24	2.980	4	0	0	52.600	3
VI	250.25	4.210	2	0	0	34.140	2
VII	347.24	3.000	2	0	0	34.140	1
VIII	278.21	3.320	4	0	0	43.370	2
IX	303.14	2.610	4	1	0	63.600	2
X	303.14	2.580	3	1	0	54.370	1
XI	310.31	4.050	5	0	0	34.140	2
XII	250.25	3.310	3	0	0	43.370	3
XIII	259.26	4.060	2	0	0	34.140	1
XIV	284.7	4.080	2	0	0	34.140	1
XV	286.69	2.950	4	0	0	60.440	3

Table5: Pharmacokinetic properties most active derivatives of Indane 1.3 dione

Comp. No	MR	logKp (cm/s)	GI absorption	BBB permeant	Pgp substrate	CYP1A2 inhibitor	CYP2C19 inhibitor	CYP2C9 inhibitor
I	49.91	-6.76	High	Yes	0.9880	Yes	Yes	Yes
II	74.49	-5.05	High	Yes	0.8056	Yes	Yes	Yes
IV	78.34	-5.64	High	No	0.9525	Yes	Yes	Yes

V	74.53	-5.01	High	Yes	0.8289	Yes	Yes	Yes
VI	82.51	-5.65	High	Yes	0.9211	Yes	Yes	Yes
VII	88.79	-4.40	High	Yes	0.9399	Yes	Yes	Yes
VIII	69.52	-5.24	High	Yes	0.9844	Yes	Yes	Yes
IX	75.97	-5.49	High	Yes	0.9347	Yes	Yes	Yes
X	78.04	-5.79	High	Yes	0.8704	Yes	Yes	Yes
XIII	80.82	-5.27	High	Yes	0.9616	Yes	Yes	Yes
XIV	79.54	-4.77	High	Yes	0.9851	Yes	Yes	Yes

The results for all derivatives that follow the Veber parameters and Lipinski's rule of five are shown Table 4. Produced series has good drug-like qualities, as shown by their log of octanol/water partition coefficient < 5, hydrogen bond acceptor counts < 5, and hydrogen bond donor counts < 10 , MW≤ 500 Da is their molecular weight. Furthermore, a number of metrics were computed, such as the topological polar surface area and the number of rotatable bonds .The TPSA values range from 34.140 to 79.960 Å2 and are greater than 60 Å2 but less than 140 Å2. Compounds III, IX, and XV have poor blood–brain barrier penetration, as indicated by TPSA values larger than 60 Å2. On the other hand, the excellent intestine absorption is indicated by values less than 140 Å2.Number of rotatable bonds assesses the molecular flexibility of the molecule; a value within < 10 indicates this. TFor the planned derivatives, the anticipated nRotB ranges are 1 to 3. Since no derivative was found to break more than one Lipinski criterion, it appears that the recommended compounds had high oral absorption.Based on the computed in silico ADME values, it was determined that the skin permeability of the design variants was within allowed range -8.0 to -1.0 cm/s . The measurement of an atom's or a collection of atoms' volume as indicated by their molar refractivity. The molar refractivity values of intended derivatives vary from 49.91 to 88.79, which is within the advised range of 40–130.With the exception of Compound IV, all developed derivatives exhibit significant gastrointestinal absorptions and are capable of penetrating the BBB, according to Table 4's research. As a result, treatment of cerebral malaria for indane dione derivatives is made successful.The results of the inhibitory prediction, drug likelihood, and the in-silico ADME predictions for the three Cytochrome P450 (CYP) isoforms: CYP2C9, CYP2C19, and CYP1A2. These forecasts show that all of the tests pass when they are investigated.

MOLECULAR DOCKING RESULT:

The malarial targets, 1LEE and 1LDG, were used in a molecular docking analysis. The amount of hydrogen bonds formed and the potential Indane dione derivatives' binding affinities to the malarial protein target are displayed in Table 6. A study on molecular docking was conducted With respect to the conventional medication chloroquine (which has binding affinity -5.8 kcal/mol), Good affinity is shown by all the derivatives, which range from - 6.9 kcal/mol for 1LEE to -7.6 kcal/mol for 1LDG.Indane derivatives docking with 1LDG shows that Compound XIII showed best docking results with good binding affinity -8.4 kcal/mol, amino acid residues found Ile119,Ala98,Ile54,Ala98,Phe100 and possessed zero hydrogen bonds and the interaction profile is dominated by the hydrophobic interactions, particularly with Ala98 represented in (Table 7). Other compounds named II, V, VII, X shows equal binding affinity -8.1 kcal/mol.The amino acid residues found with Compound II are Lys118, Ile119, Ala98, Ile54 showing Pi-Alkyl, Pi-Sigma interactions. Compound V interact with amino acid residues Phe100, Ile119, Ala98 displaying interactions between Pi-Alkyl, Pi-Pi, Pi-Alkyl, and Pi-Sigma. The aminoacid residues found with Compound VII are Arg171, Tyr174, Lys173, Arg185 showing Pi-Alkyl,

Pi-Pi-T-Shaped, Pi-Pi interactions and possessed one hydrogen bond with Arg185.Compound X interact with amino acid residues Phe100, Ile119, Ala98, Ile54 showing Pi-Alkyl, Pi-Alkyl, Pi-Sigma interactions. On basis of molecular docking analysis of designed Indane 1.3 dione derivatives, we can say that all the compound showed good docking interactions with 1LDG as compared to standard drug Chloroquine and only compound VII forms one hydrogen bond with Arg185 have a potential to become a lead.
Indane derivatives docking with 1LEE shows that Compound I,III and VII showed best docking results with good binding affinity -7.8 kcal/mol, amino acid residues found are Met 15,Phe120,Ile32,Val78,Gly216,Asp34 and showing Pi-Pi-T-Shaped, Pi-Alkyl interactions represented in (Table 8).Compound IV, XIII, XIV shows equal binding affinity -7.5 kcal/mol. The amino acid residues found with Compound IV are Arg 307,Tyr272,Lys327,Val160,Lys163 showing Pi-Alkyl, Pi-Cation donor interactions and possessed two conventional H-Bond with Arg 307,Tyr272.
Compound VI,VIII shows binding affinity -7.4 kcal/mol which have interacted with amino acids namely Val141,Lys129,Trp128,Asp130,Asp190 showing Alkyl, Pi-Alkyl, Pi-anion inteactions with two conventional H-bonds Compound VI represented in (Table 5).Whereas Compound VIII interacts with amino acids Leu324,Pro181,Tyr266,Ile322,Tyr309,Thr183, Asn263 showing Pi-Alkyl, Alkyl, Pi-Pi-T-Shaped interactions by forming five Conventional-H bonds.
On the basis of molecular docking analysis of designed Indane 1,3 dione , we can say that Compound I,III,VII,IV,XIII,XIV showed good docking interactions with 1LEE and these compounds have a potential to become a lead.From this study we can conclude that out of these two drug targets 1LDG and 1LEE the designed Indane dione derivatives shows good binding interactions with 1LEE compared to 1LDG as more hydrogen bond formation shown by compounds IV,VI,VIII,XIII,XV.

Table 6: Binding affinities for 1LDG and 1LEE with the designed Indane 1.3 dione derivatives

Sr. No	Ligand	Binding Affinity (Kcal / mol)	Binding Affinity (Kcal / mol)	Sr. No	Ligand	Binding Affinity (Kcal / mol)	Binding Affinity (Kcal / mol)	Sr. No	Ligand	Binding Affinity (Kcal / mol)	Binding Affinity (Kcal / mol)
		1LDG	1LEE			1LDG	1LEE			1LDG	1LEE
	I	- 8.2	-7.8	7.	VII	-8.1	-7.8	13.	XIII	-8.4	-7.5
	II	- 8.1	-7.3	8.	VIII	-7.7	-7.4	14.	XIV	-8	-7.5
	III	-8.1	-7.8	9.	IX	-8.2	-7.2	15.	XV	-8	-6.9
	IV	-7.6	-7.5	10.	X	-8.1	-7.3	16.	Chloroquine	-5.8	-5.8
	V	-8.1	-7.3	11.	XI	-8	-7.4				
	VI	-7.9	-7.4	12.	XII	-7.7	-6.9				

Table 7: Molecular interactions of INDANE 1, 3 DIONE Derivatives with 1LEE and 1LDG

Receptor Name	Comp.Code	Binding Affinity (kcal / mol)	No. H Bond	Interacting Amino acids	Bond Distance (Å)	Type of Interaction
Aspartic protease plasmepsin II (PDB:1LEE)	I	-7.8	0	Met 15 Phe120 Ile32 Val78 Gly216 Asp34 Asp34 Asp34	5.31 4.99 5.02 5.24 3.40,3.61 4.78 4.74 4.64	Alkyl Pi Pi- T- Shaped Pi Alkyl Pi Alkyl Fluorine Pi anion Pi anion Pi anion

	IV	-7.5	1	Ile32 Ile32 Tyr77 Ile123 Val78 Val78 SER37 Asp214 Asp214 Asp34	4.79 3.57 5.75 5.09 3.97 5.08 3.60 3.84 4.38 4.86	Pi Alkyl Alkyl PiPi T -Shaped Pi Alkyl Pi Sigma Pi Alkyl Carbon H -Bond Pi anion Pi anion Pi anion
	VI	-7.4	2	Val141 Val141 Lys129 Trp128 Asp130 Asp190 Asp190	5.00 4.51 5.13 5.10 2.17 2.61 4.28 3.50	Alkyl Alkyl Pi Alkyl Pi Pi -T-Shaped Conventional H- Conventional H- Pi anion Pi anion
	VIII	-7.4	5	Leu324 Leu324 Pro181 Tyr266 Ile322 Ile322 Ile322 Tyr309 Thr183 Asn263	4.00 3.88 5.12 4.38 5.53 2.49 2.50 2.82 2.52 2.60 3.58	Pi Alkyl Pi Alkyl Pi Alkyl Alkyl Pi Pi - T-Shaped Conventional -H Conventional -H Conventional -H Conventional -H Conventional -H Carbon
	XIII	-7.5	1	Ile277 Ile277 Ile277 Tyr272 Val160 Tyr272 Tyr272 Tyr272 Tyr272 Arg307	4.77 3.59 3.80 5.02 3.87 5.17 5.02 5.50 5.10 2.10	Pi Alkyl Alkyl Alkyl Pi Alkyl Pi Sigma Pi Alkyl Pi Alkyl Pi Pi T-Shaped PiPi -T-Shaped Conventional H
	XIV	-7.5	1	Ile277 Ile277 Arg307 Val160 Val160 Tyr272 Tyr272 Arg307	3.56 4.80 5.16 5.00 3.86 5.11 5.49 2.07	Alkyl Pi Alkyl Pi Alkyl Pi Alkyl Pi-Sigma Pi Pi-T-Shaped Pi Pi-T-Shaped Conventional-H
	CHL	-5.8	1	Thr217 Val78 Val78 Tyr77	3.02 4.98 4.50 3.90	Pi-Donor-H Pi Alkyl Pi Alkyl Pi Sigma
	II	-8.1	0	Lys118	5.09	Pi Alkyl

Plasmodium falciparum lactate dehydrogenase (PfLDH) (PDB:1LDG)				Ile119 Ile119 Ala98 Ala98 Ala98 Ile54 Ile54	4.74 4.48 4.46 3.54 3.94 3.83 3.86	Pi Alkyl Pi Alkyl Pi Alkyl Pi Sigma Pi Sigma Pi Sigma Pi Sigma
	V	-8.1	0	Phe100 Phe100 Ile119 Ala98 Ala98 Ile54 Ile54	3.91 4.15 4.98 3.48 4.29 3.87 3.93	Pi Alkyl Pi Pi Staked Pi Alkyl Pi Sigma Pi Alkyl Pi Sigma Pi Alkyl
	VII	-8.1	1	Arg171 Tyr175 Tyr174 Tyr174 Lys173 Arg185 Arg185 Arg185 Pro184	5.33 5.56 4.19 5.20 4.45 2.42 3.37 3.60 3.63	Pi Alkyl Pi Pi-T-Shaped Pi Pi Staked Pi Pi Staked Alkyl Conventional-H Carbon Carbon fluorine Fluorine
	IX	-8.2	0	Ala98 Ala98 Phe100 Phe100 Phe100 Ile54 Ile54 Ile119	3.50 4.33 4.14 3.96 5.00 3.85 3.93 4.97	Pi Sigma Pi Alkyl Pi Pi Staked Pi Alkyl Pi Alkyl Pi Sigma Pi Alkyl Pi Alkyl
	X	-8.1	0	Ile119 Ile119 Ile54 Ala98 Ala98 Phe100 Phe100	4.98 3.93 3.87 3.48 4.29 4.15 3.94	Pi Alkyl Pi Alkyl Pi Sigma Pi Sigma Pi Alkyl Pi Pi Staked Pi Alkyl
	XIII	-8.4	0	Ile119 Ala98 Ile54 Ala98 Phe100	4.90 4.32 3.82 3.51 4.15	Pi Alkyl Pi Alkyl Pi Sigma Pi Sigma Pi Pi Staked
	XV	-8	0	Glu122 Glu122 Lys118 Ile119 Ile119 Ile54 Ile54 Ille54 Ala98	3.11 3.00 3.81 4.78 4.51 3.91 3.83 3.88 3.54	Fluorine Fluorine Alkyl Pi Alkyl Pi Alkyl Pi Sigma Pi Sigma Pi Sigma Pi Sigma

					4.53	Pi Alkyl
	CHL	-5.8	0	Lys118 Ile119 Ile123 Tyr85 Val26 Ile123 Ala98 Ile54 Ile54 Ile54 Ala98 Ala98	4.03 5.01 5.30 5.02 5.12 4.43 4.00 4.48 4.98 4.01 3.81 5.10	Alkyl Pi Alkyl Alkyl Pi Alkyl Alkyl Pi Alkyl Alkyl Alkyl Pi Alkyl Pi Alkyl Pi Sigma Pi Alkyl

In Vitro Antimalarial Activity

The produced compounds' (I–XV) in vitro antimalarial activity is listed in the table below. Out of the fifteen compounds examined, three (XI, XII, and XIV) showed that it was able to inhibit Schizonts at a half-maximal inhibitory concentration (IC_{50}) of less than 0.5 µM, or <500 nM. According to the in vitro antimalarial activity data compounds I, V, VII, VIII, X, XIII, and XV displayed moderate activity according to the IC_{50} values, while compounds II, III, IV, VI, and IX demonstrated less activity.The IC_{50} values and % inhibition of compounds I to XV are presented in below table 8.

Table 8: In vitro antimalarial activity of Compounds I to XV

Compound No	Concentration	No. of Schizonts/200parasites	% inhibition	IC_{50}	
				µg/mL	µM
I	Chloroquine	135	100	17.54	39.20
	2	125	94		
	4	120	89		
	8	105	78		
	16	75	56		
	32	33	24		
	64	0	0		
	128	0	0		
II	Chloroquine	132	100	32.14	64.12
	2	128	95		
	4	119	89		
	8	107	80		
	16	81	58		
	32	31	23		
	64	0	0		
	128	0	0		
III	Chloroquine	134	100	31.25	62.45
	2	129	96		
	4	124	93		
	8	118	84		
	16	93	69		
	32	51	39		
	64	0	0		
	128	0	0		
IV	Chloroquine	136	100	30.24	60.45
	2	132	97		

	4	127	93		
	8	118	87		
	16	101	74		
	32	66	48		
	64	0	0		
	128	0	0		
V	Chloroquine	132	100	18.02	36.24
	2	129	97		
	4	124	94		
	8	116	88		
	16	99	75		
	32	72	55		
	64	0	0		
	128	0	0		
VI	Chloroquine	137	100	35.39	70.03
	2	129	93		
	4	121	88		
	8	102	74		
	16	68	50		
	32	0	0		
	64	0	0		
	128	0	0		
VII	Chloroquine	133	100	13.10	25.12
	2	121	91		
	4	115	86		
	8	91	68		
	16	55	43		
	32	0	0		
	64	0	0		
	128	0	0		
VIII	Chloroquine	135	100	13.45	27.46
	2	99	73		
	4	60	44		
	8	0	0		
	16	0	0		
	32	0	0		
	64	0	0		
	128	0	0		
IX	Chloroquine	137	100	33.12	66.96
	2	102	74		
	4	67	49		
	8	0	0		
	16	0	0		
	32	0	0		
	64	0	0		
	128	0	0		
X	Chloroquine	133	100	12.63	24.02
	2	91	69		
	4	58	43		
	8	0	0		

	16	0	0		
	32	0	0		
	64	0	0		
	128	0	0		
XI	Chloroquine	137	100	9.33	19.36
	2	111	90		
	4	108	80		
	8	80	58		
	16	37	26		
	32	0	0		
	64	0	0		
	128	0	0		
XII	Chloroquine	134	100	9.56	18.67
	2	120	90		
	4	107	80		
	8	79	59		
	16	38	28		
	32	0	0		
	64	0	0		
	125	0	0		
XIII	Chloroquine	136	100	16.28	30.04
	2	127	94		
	4	120	88		
	8	103	76		
	16	72	53		
	32	0	0		
	64	0	0		
	128	0	0		
XIV	Chloroquine	134	100	9.23	17.45
	2	129	96		
	4	122	93		
	8	115	86		
	16	97	72		
	32	59	44		
	64	0	0		
	128	0	0		
XV	Chloroquine	136	100	12.14	25.09
	2	125	92		
	4	114	84		
	8	93	68		
	16	50	37		
	32	0	0		
	64	0	0		
	128	0	0		

Table 9: A molecular interaction between Indane 1,3 dione derivatives and 1LDG: (a) binding location in the 1LDG active site ; (b) the kind of compound interaction that attaches to 1LDG's amino acids.

	1LDG:Interaction with Indane 1,3 dione derivatives		**1LEE:Interaction between Indane 1,3dione derivatives**

Comp ID	3D	2D	Comp ID	3D	2D
II	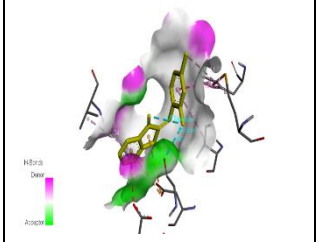	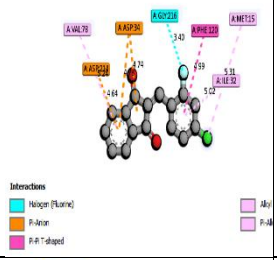	II	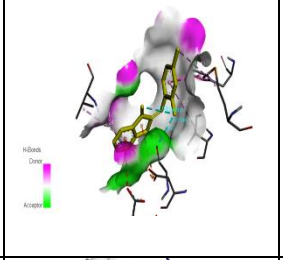	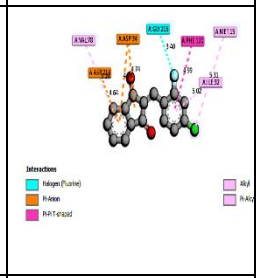
V	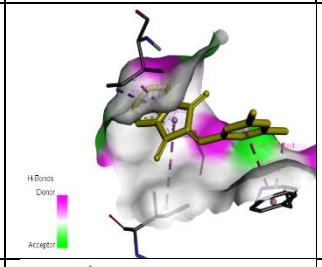	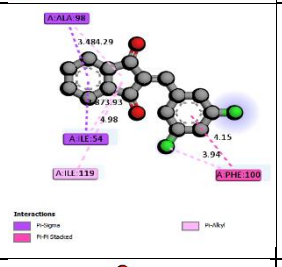	V	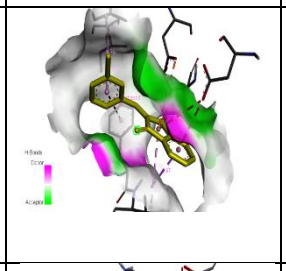	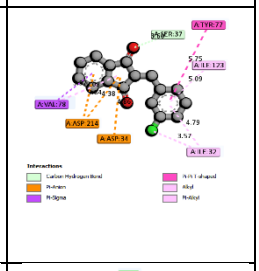
VII	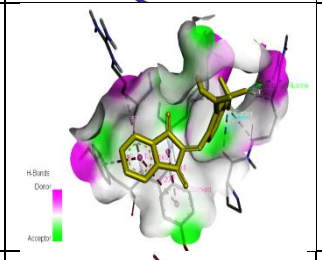	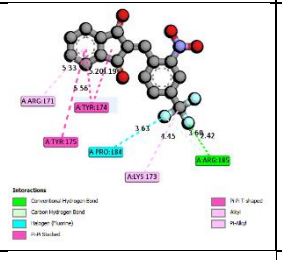	VII	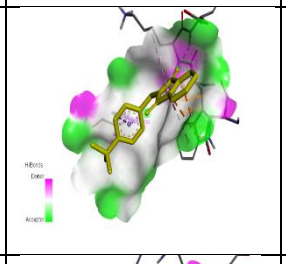	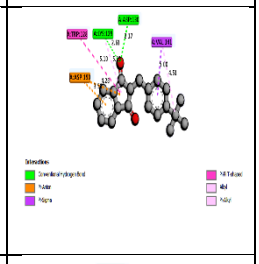
IX	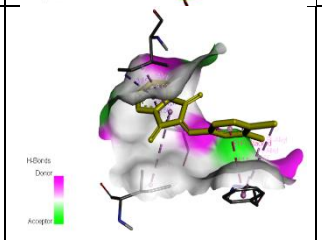	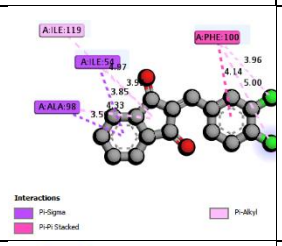	IX	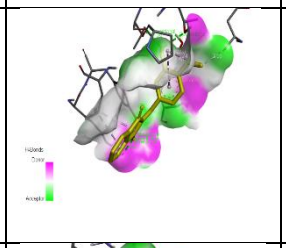	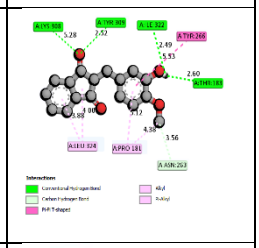
XIV	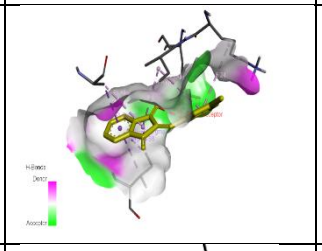	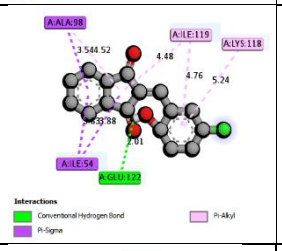	XIV	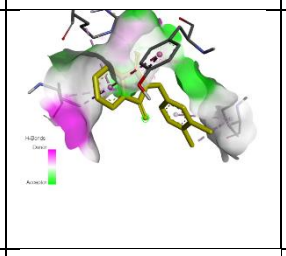	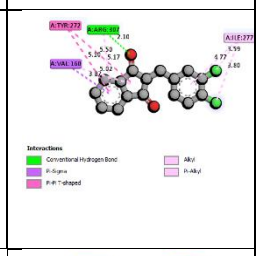
XV	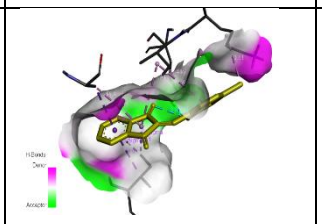	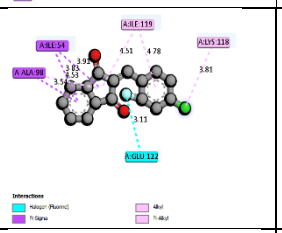	XV	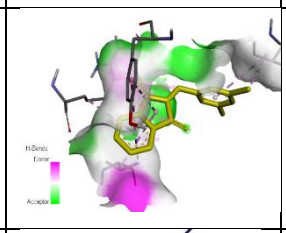	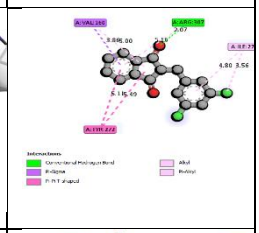
CHL	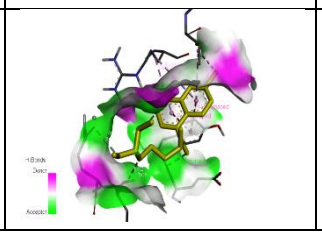	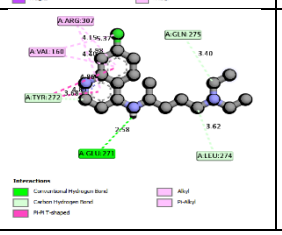	CHL	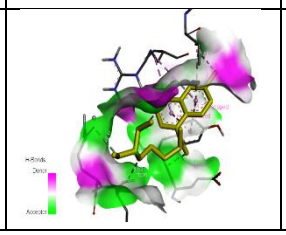	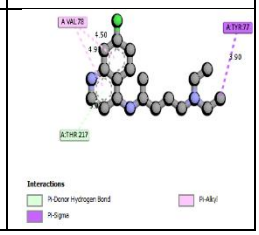

CONCLUSION

Plasmodium falciparum lactate dehydrogenase (Pf-LDH) (PDB:1LDG) and Aspartic protease plasmepsin II (PDB:1LEE) are the two possible therapeutic targets that might be taken into consideration while developing antimalarial drugs to tackle the malaria problem. The design and prediction of possible interaction mechanisms and binding affinities of indane 1,3 dione substituted compounds with 1LEE and 1LDG are explained by this work. Among the designed ligands with 1LDG, Compound XIII had the greatest dock score value, while among those with 1LEE, Compound II had the highest docking score value.Good in silico ADMET qualities were possessed by all the proposed compounds, indicating their safety for future synthesis and development into effective antimalarial medicines that are commercially available. The current work demonstrated the molecular docking analysis of Indane 1.3 dione derivatives and its antimalarial assessment against the P. falciparum 3D7 strain, which is susceptible to chloroquine. According to the results, compound XI, compound XII, and compound XIV are the most potent derivatives with significant in vitro antimalarial activity against Schizonts with half maximal inhibitory concentrations (IC_{50}) values less than 0.5 μM (i.e.<500 nM). These compounds may also provide a lead for discovery of a new class Pf -LDH inhibitor.

Conflict Of Interest

There is no conflict of interest in this work, according to the author.

REFERENCES:

1.Who.int, https://www.who.int/teams/global-malaria-programme/reports/world-malaria-report-2022. Accessed 15 Oct. 2024.
2.Ya'u Ibrahim, Zakari, et al. "Molecular Docking Studies, Drug-Likeness and in-Silico ADMET Prediction of Some Novel β-Amino Alcohol Grafted 1,4,5-Trisubstituted 1,2,3-Triazoles Derivatives as Elevators of P53 Protein Levels." Scientific African, vol. 10, no. e00570, 2020, p. e00570, doi:10.1016/j.sciaf.2020.e00570.
3.World Health Organization (WHO). WHO guidelines for malaria. Geneva: World Health Organization; 2023 Mar 14 https://www.who.int/publications/i/item/9789240068925.
4.Wicht, Kathryn J., et al. "Molecular Mechanisms of Drug Resistance in Plasmodium Falciparum Malaria." Annual Review of Microbiology, vol. 74, no. 1, 2020, pp. 431–454, doi:10.1146/annurev-micro-020518-115546.
5.Pasupureddy, Rahul, et al. "Current Scenario and Future Strategies to Fight Artemisinin Resistance." Parasitology Research, vol. 118, no. 1, 2019, pp. 29–42, doi:10.1007/s00436-018-6126-x.
6.Zhang, Yinliang, et al. "The Plasmodium Falciparum Drugome And Its Polypharmacological Implications." bioRxiv, 2016, doi:10.1101/042481.
7.Chu, Cindy S., and Nicholas J. White. "Management of Relapsing Plasmodium Vivax Malaria." Expert Review of Anti-Infective Therapy, vol. 14, no. 10, 2016, pp. 885–900, doi:10.1080/14787210.2016.1220304.
8.Ji, Xin, et al. "In Silico and in Vitro Antimalarial Screening and Validation Targeting Plasmodium Falciparum Plasmepsin V." Molecules (Basel, Switzerland), vol. 27, no. 9, 2022, p. 2670, doi:10.3390/molecules27092670.
9.Vaughan, Ashley M., et al. "Malaria Parasite Pre-Erythrocytic Stage Infection: Gliding and Hiding." Cell Host & Microbe, vol. 4, no. 3, 2008, pp. 209–218, doi:10.1016/j.chom.2008.08.010.
10. Egan, Timothy J. "Haemozoin Formation." Molecular and Biochemical Parasitology, vol. 157, no. 2, 2008, pp. 127–136, doi:10.1016/j.molbiopara.2007.11.005.
11. Klemba, Michael, and Daniel E. Goldberg. "Characterization of Plasmepsin V, a Membrane-Bound Aspartic Protease Homolog in the Endoplasmic Reticulum of Plasmodium Falciparum." Molecular and Biochemical Parasitology, vol. 143, no. 2, 2005, pp. 183–191, doi:10.1016/j.molbiopara.2005.05.015.
12. Russo, Ilaria, et al. "Plasmepsin V Licenses Plasmodium Proteins for Export into the Host Erythrocyte." Nature, vol. 463, no. 7281, 2010, pp. 632–636, doi:10.1038/nature08726.
13. Ecker, Andrea, et al. "Reverse Genetics Screen Identifies Six Proteins Important for Malaria Development in the Mosquito: Proteins Important for Malaria Development in the Mosquito." Molecular Microbiology, vol. 70, no. 1, 2008, pp. 209–220, doi:10.1111/j.1365-2958.2008.06407.x.
14. Li, Fengwu, et al. "Plasmodium Falciparum Ookinete Expression of Plasmepsin VII and Plasmepsin X." Malaria Journal, vol. 15, no. 1, 2016, p. 111, doi:10.1186/s12936-016-1161-5.
15. Mastan, Babu S., et al. "Plasmodium Berghei Plasmepsin VIII Is Essential for Sporozoite Gliding Motility." International Journal for Parasitology, vol. 47, no. 5, 2017, pp. 239–245, doi:10.1016/j.ijpara.2016.11.009.
16. Nasamu, Armiyaw S., et al. "Plasmepsins IX and X Are Essential and Druggable Mediators of Malaria Parasite Egress and Invasion." Science (New York, N.Y.), vol. 358, no. 6362, 2017, pp. 518–522, doi:10.1126/science.aan1478.
17. Sussman, Fredy, et al. "On the Active Site Protonation State in Aspartic Proteases: Implications for Drug Design." Current Pharmaceutical Design, vol. 19, no. 23, 2013, pp. 4257–4275, doi:10.2174/1381612811319230009.
18. Fatimawali, et al. "Appraisal of Bioactive Compounds of Betel Fruit as Antimalarial Agents by Targeting Plasmepsin 1 and 2: A Computational Approach." Pharmaceuticals (Basel, Switzerland), vol. 14, no. 12, 2021, p. 1285, doi:10.3390/ph14121285.
19. Gowthaman, Ramasamy, et al. "A Database for Plasmodium Falciparum Protein Models." Bioinformation, vol. 1, no. 2, 2005, pp. 50–51, doi:10.6026/97320630001050.

20. Plouffe, David, et al. "In Silico Activity Profiling Reveals the Mechanism of Action of Antimalarials Discovered in a High-Throughput Screen." Proceedings of the National Academy of Sciences of the United States of America, vol. 105, no. 26, 2008, pp. 9059–9064, doi:10.1073/pnas.0802982105.
21. Bobrovs, Raitis, et al. "Exploring Aspartic Protease Inhibitor Binding to Design Selective Antimalarials." Journal of Chemical Information and Modeling, vol. 62, no. 13, 2022, pp. 3263–3273, doi:10.1021/acs.jcim.2c00422.
22. Ribbiso, Kaleab A., et al. "Artemisinin-Based Drugs Target the Plasmodium Falciparum Heme Detoxification Pathway." Antimicrobial Agents and Chemotherapy, vol. 65, no. 4, 2021, doi:10.1128/AAC.02137-20.
23. Kayamba, Francis, et al. "Lactate Dehydrogenase and Malate Dehydrogenase: Potential Antiparasitic Targets for Drug Development Studies." Bioorganic & Medicinal Chemistry, vol. 50, no. 116458, 2021, p. 116458, doi:10.1016/j.bmc.2021.116458.
24. Singh, R., et al. "Identification of a Novel Binding Mechanism of Quinoline-Based Molecules with Lactate Dehydrogenase of Plasmodium Falciparum." J Biomol Struct Dyn, vol. 39, no. 1, 2021, pp. 348–356, doi:10.1080/07391102.2020.1711809.
25. Joshi, Nishant, et al. "Highly Potent Anti-Malarial Activity of Benzopyrano(4,3-b)Benzopyran Derivatives and in Silico Interaction Analysis with Putative Target Plasmodium Falciparum Lactate Dehydrogenase." Journal of Biomolecular Structure & Dynamics, vol. 40, no. 11, 2022, pp. 5159–5174, doi:10.1080/07391102.2020.1868336.
26. Chaniad, Prapaporn, et al. "Antimalarial Potential of Compounds Isolated from Mammea Siamensis T. Anders. Flowers: In Vitro and Molecular Docking Studies." BMC Complementary Medicine and Therapies, vol. 22, no. 1, 2022, p. 266, doi:10.1186/s12906-022-03742-7.
27. Samad, Abdus, et al. "Designing a Multi-Epitope Vaccine against SARS-CoV-2: An Immunoinformatics Approach." Journal of Biomolecular Structure & Dynamics, vol. 40, no. 1, 2022, pp. 14–30, doi:10.1080/07391102.2020.1792347.
28. Anderson, Amy C. "The Process of Structure-Based Drug Design." Chemistry & Biology, vol. 10, no. 9, 2003, pp. 787–797, doi:10.1016/j.chembiol.2003.09.002.
29. Ertl, P., et al. "Fast Calculation of Molecular Polar Surface Area as a Sum of Fragment-Based Contributions and Its Application to the Prediction of Drug Transport Properties." Journal of Medicinal Chemistry, vol. 43, no. 20, 2000, pp. 3714–3717, doi:10.1021/jm000942e.
30. O'Boyle, Noel M., et al. "Open Babel: An Open Chemical Toolbox." Journal of Cheminformatics, vol. 3, no. 1, 2011, p. 33, doi:10.1186/1758-2946-3-33.
31. Yoshikawa, Naruki, and Geoffrey R. Hutchison. "Fast, Efficient Fragment-Based Coordinate Generation for Open Babel." Journal of Cheminformatics, vol. 11, no. 1, 2019, p. 49, doi:10.1186/s13321-019-0372-5.
32. Berman, Helen M., et al. "The Protein Data Bank." Acta Crystallographica. Section D, Biological Crystallography, vol. 58, no. 6, 2002, pp. 899–907, doi:10.1107/s0907444902003451.
33. Sharma, R., and D. Chetia. "Docking Studies on Quinine Analogs for Plasmepsin-II of Malaria Parasite Using Bioinformatics Tools." Int J Pharm Pharm Sci, vol. 5, 2013, pp. 681–685.
34. "Dassault Systèmes, BIOVIA Discovery Studio Visualizer V21.1.0.20298." BIOVIA, 2021.
35. Dallakyan, Sargis, and Arthur J. Olson. "Small-Molecule Library Screening by Docking with PyRx." Methods in Molecular Biology, Springer New York, 2015, pp. 243–250.
36. Laskowski, Roman A. "PDBsum1: A Standalone Program for Generating PDBsum Analyses." Protein Science: A Publication of the Protein Society, vol. 31, no. 12, 2022, doi:10.1002/pro.4473.
37. Daina, Antoine, et al. "SwissADME: A Free Web Tool to Evaluate Pharmacokinetics, Drug-Likeness and Medicinal Chemistry Friendliness of Small Molecules." Scientific Reports, vol. 7, no. 1, 2017, doi:10.1038/srep42717.
38. Ritchie, Timothy J., et al. "The Graphical Representation of ADME-Related Molecule Properties for Medicinal Chemists." Drug Discovery Today, vol. 16, no. 1–2, 2011, pp. 65–72, doi:10.1016/j.drudis.2010.11.002.
39. Egan, W. J., et al. "Prediction of Drug Absorption Using Multivariate Statistics." Journal of Medicinal Chemistry, vol. 43, no. 21, 2000, pp. 3867–3877, doi:10.1021/jm000292e.
40. Ara, N., et al. "A Strategy to Enhance Bioavailability of Drug Candidates: Natural Bioenhancers." Int J Pharm Bio Med Sci, vol. 1, 2021, pp. 10–14.
41. Daina, Antoine, and Vincent Zoete. "A BOILED-Egg to Predict Gastrointestinal Absorption and Brain Penetration of Small Molecules." ChemMedChem, vol. 11, no. 11, 2016, pp. 1117–1121, doi:10.1002/cmdc.201600182.
42. Ambudkar, Suresh V., et al. "P-Glycoprotein: From Genomics to Mechanism." Oncogene, vol. 22, no. 47, 2003, pp. 7468–7485, doi:10.1038/sj.onc.1206948.
43. Sharom, F. J. "The P-Glycoprotein Efflux Pump: How Does It Transport Drugs?" The Journal of Membrane Biology, vol. 160, no. 3, 1997, pp. 161–175, doi:10.1007/s002329900305.
44. Lipinski, C. A. "Lead- and Drug-like Compounds: The Rule-of-Five Revolution." Discov Today Technol, vol. 1, no. 4, 2004, pp. 337–341, doi:10.1016/j.ddtec.2004.11.00.
45. Londhe, N. A., and K. Krishnan. "Eur Chem Bull." Eur Chem Bull, vol. 12, no. 7, 2023, pp. 5958–5969, doi:10.48047/ecb/2023.12.si7.5202023.23/09/2023.
46. Trager, William, and James B. Jensen. "Human Malaria Parasites in Continuous Culture." Science (New York, N.Y.), vol. 193, no. 4254, 1976, pp. 673–675, doi:10.1126/science.781840.